Fatigue analysis of large slewing bearing using strain-life approach

R. Potočnik[1,], J. Flašker[1], S. Glodež[2]*
[1]University of Maribor, Faculty of Mechanical Engineering, Maribor, Slovenia;
[2]University of Maribor, Faculty of Natural Sciences and Mathematics,Maribor, Slovenia

**Corresponding author: roki.potocnik@uni-mb.si*

Abstract

Large slewing bearings are designed to sustain axial, radial and tilting moments. Due to their design and manufacturing process, a nonstandard approach has to be used to calculate the fatigue life. First, a maximum contact force is obtained from the load distribution in a bearing by means of analytical expressions of the Hertzian contact theory. Then, a strain-life approach is used to calculate the fatigue life on the basis of the subsurface stresses as obtained from the finite element analysis. Experimentally determined depth-dependent elasto-plastic material properties, which appear as a result of hardening, are taken into consideration. The fatigue life largely depends on external bearing loads. For an external loading, which results in 3200 MPa contact pressure on a bearing raceway, the fatigue life is approximately 4.69e7 load cycles (1.54e6 revolutions). The calculated fatigue life is in accordance with the requirements of the fatigue life of wind turbines' blade flange bearings.

Keywords: fatigue, large rolling bearing, strain-life, elasto-plastic

1. Introduction

Slewing bearings are machine elements which enable relative rotation of two structural parts, as shown in Fig. 1. They can accommodate axial (F_a), radial (F_r) and tilting moment loads (M) acting either singly or in combination and in any direction as shown in **Fig. 1**. The bearings are made of inner and outer rings, rolling elements and spacers, which prevent rolling elements from hitting against each other. The rings are typically available in one of three executions: a) without

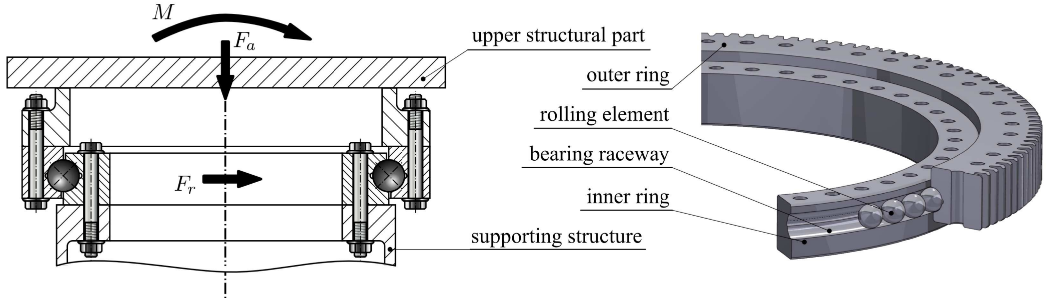

Fig. 1: Typical slewing bearing assembly and loading conditions

gears, b) with an internal gear and c) with an external gear. Slewing bearings can perform both oscillating (slewing) and rotating movements. The rotational speed usually ranges from 0.1 to 5 rpm. They are widely used in construction of transport devices (cranes, transporters, turning tables, etc.), wind turbines production and other fields of mechanical engineering.

The calculation of load capacity of “standard” bearings is widely known and standardized [1]. It is based on the Hertzian theory of contact, statistical approach and a vast number of tests, which are used to determine different “Life Adjustment Factors” [1,2,3]. Since the manufacturing process and operating conditions of large bearings significantly differ from those for standard bearings, the load capacity of such bearings usually can not be determined using the standardized procedure. Hence, a rather simple, and a well known strain-life approach for the calculation of fatigue life is presented in the paper. Furthermore, special attention is being paid to the material properties of the bearing raceway. The calculation procedure in this paper is carried out for a four contact-point single row rolling bearing.

2. Fatigue analysis

2.1. Loads

The bearing is typically loaded with the axial force F_a, radial force F_r, and tilting moment M, as shown in **Fig. 1**. These loads are carried over to the bearing raceways by rolling elements, which usually results in the non-uniform contact loading of the raceways. However, since the rotating speeds of large slewing bearings are usually rather small, the rolling and friction is not taken into consideration. Therefore, the only loads acting on the raceway are the contact forces Q_i, where i stands for the i-th rolling element, as shown in **Fig. 2a**. For the purpose of the fatigue analysis, only the maximum contact force $Q_{\max}$, obtained from the contact load distribution as described in [4], is taken into account. Moreover, due to the nature of the problem, the contact force is assumed to be pulsating, as shown in **Fig. 2**. Hence, the mean and amplitude contact forces, Q_m and Q_a, respectively, are calculated as:

$$Q_m = Q_a = Q_{\max}/2 \quad . \tag{1}$$

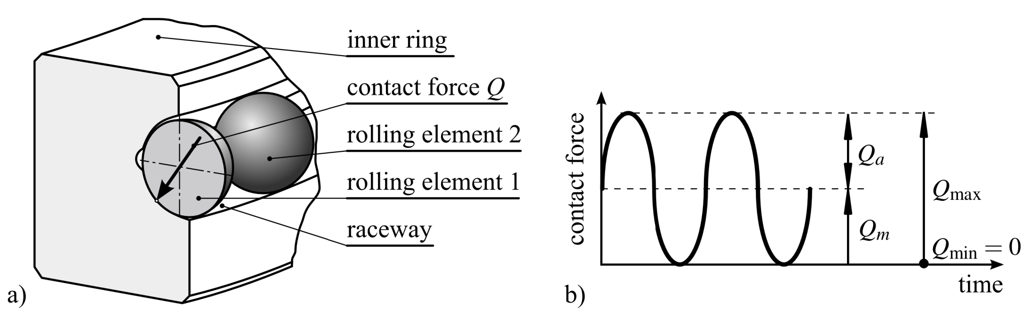

Fig. 2: a) Contact force acting on the bearing raceway, and b) pulsating loading

2.2. Material properties

The presented approach assumes that the raceways and rolling elements can be modeled with elasto-plastic and elastic material properties, respectively. According to the in-house research and experimental work the rolling elements, if loaded with the usual contact forces, do not undergo plastic deformations. On the contrary, the bearing rings are made of somehow “weaker” material. Since the manufacturing procedure includes surface hardening, the raceways usually have rather hard case and ductile core. This means that at higher contact loads plastic deformations below the surface can appear. Hence, the material characteristics of the raceway change with the depth.

By taking into observation the above mentioned, the bearing raceway is divided into layers with different elasto-plastic material properties. The layers are defined on the basis of the measured depth-dependent hardness profile, which means that each layer has different hardness. Furthermore, each layer is modeled with the cyclic stress-strain curve characterized by a Ramberg-Osgood equation [5]:

$$\varepsilon_a = \frac{\Delta\varepsilon}{2} = \frac{\Delta\varepsilon_e}{2} + \frac{\Delta\varepsilon_p}{2} = \frac{\sigma_a}{E} + \left(\frac{\sigma_a}{K'}\right)^{1/n'} , \tag{2}$$

where ε_a, $\Delta\varepsilon_e/2$, $\Delta\varepsilon_p/2$, σ_a, E, K' and n' are true strain amplitude, true elastic strain amplitude, true plastic strain amplitude, true stress amplitude, Young's modulus of elasticity, cyclic strength coefficient and cyclic strain hardening exponent, respectively. K' and n' are calculated as [5]:

$$K' = \frac{\sigma_f'}{\left(\varepsilon_f'\right)^{b/c}} \quad \text{and} \quad n' = \frac{b}{c} , \tag{3}$$

where σ_f' and ε_f' are fatigue strength coefficient and fatigue ductility coefficient, respectively. The parameters E, b, c, σ_f' and ε_f' are obtained on the basis of the available experimental data, i.e. by averaging or by linear regression of the values available from the literature [6,7]. Similar approach has already been presented and elaborated in [8,9]. However, since mostly tensile properties are available in the literature, an assumption is made, that the material properties for the compression and tension are the same.

2.3. Subsurface stresses

Subsurface stresses are calculated on the basis of the maximum and minimum contact forces, $Q_{\max}$ and $Q_{\min}$, respectively (see **Fig. 2b**). For each of them coordinate stresses and strains, i.e. σ_{ij} and ε_{ij}, where $i,j \in \{x,y,z\}$, are obtained. It is important to take into account loading history. Stresses and strains have to be determined first at $Q_{\max}$ and only afterwards at $Q_{\min}$. This ensures that the plastic deformations, which could appear at $Q_{\max}$, are also taken into account.

Next, equivalent mean stress $\sigma_{m,q}$ and maximum alternating shear stress $\gamma_{a,\max}$ are calculated according to the following equations [5]:

$$\sigma_{m,q}=\sigma_{m,1}+\sigma_{m,2}+\sigma_{m,3} \quad \text{and} \quad \gamma_{a,\max}=\varepsilon_{a,1}-\varepsilon_{a,3} \ , \tag{4}$$

where $\sigma_{m,1}$, $\sigma_{m,2}$ and $\sigma_{m,1}$ are mean principal stresses ($\sigma_{m,1} > \sigma_{m,2} > \sigma_{m,1}$), and $\varepsilon_{a,1}$ and $\varepsilon_{,a2}$ are alternating principal strains ($\varepsilon_{a,1} > \varepsilon_{a,2}$). They are calculated as (see **Fig. 2b**):

$$\sigma_{m,i}=\frac{\sigma_{\max,i}+\sigma_{\min,i}}{2} \quad \text{and} \quad \varepsilon_{a,j}=\frac{\varepsilon_{\max,j}-\varepsilon_{\min,j}}{2} \tag{5}$$

where $i \in \{1,2,3\}$, and $j \in \{1,2\}$. The indexes i and j designate the principal values.

2.4. Number of cycles to failure

It is commonly assumed that the subsurface failures in bearings occur because of the shear stresses [3]. Therefore, the number of cycles to failure N_f is calculated according to the Tresca's hypothesis of maximum shear deformation [3,10]:

$$\gamma_{a,\max}=(1+\nu_e)\frac{\sigma_f'-\sigma_{m,q}}{E}(2N_f)^b+(1+\nu_p)\varepsilon_f'(2N_f)^c \ , \tag{6}$$

where ν_e and ν_e are elastic and plastic Poisson's ratios, respectively. **Eq. (6)** can be solved numerically by using some some iterative method. Moreover, an approximate number of bearing revolutions to failure on inner ring N_r can be calculated as [3]:

$$N_r \approx \frac{2N_f}{n_b\left(1+d_b\sin(\alpha_0/d_0)\right)} \ , \tag{7}$$

where n_b, d_b, α_0 and d_0 are number of rolling elements (balls), ball diameter, nominal contact angle of the bearing and ball track diameter, respectively.

3. Practical example

3.1. Geometry, loads and material properties

The calculation approach described above is demonstrated on the four contact-point single row ball bearing shown in **Fig. 3a**. The bearing has ball track

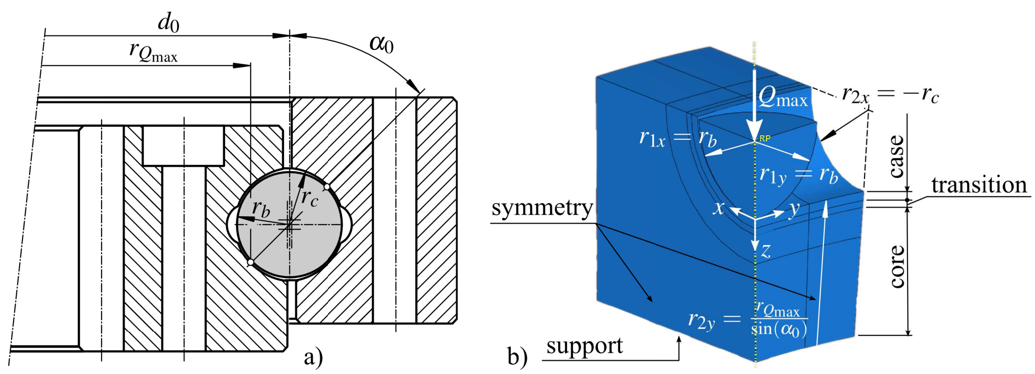

Fig. 3: a) Geometry of the bearing and b) FEM setup of the calculation

diameter $d_0 = 766$ mm, ball and raceway curvature radii $r_b = 17.5$ mm and $r_c = 18.04$ mm, respectively, nominal contact angle $a_0 = 45°$ and radial and axial clearances $c_r = 0.05$ mm and $c_a = 0.05$ mm, respectively.

Maximum contact load is calculated from the external loads $F_a = 260$ kN and $M = 290$ kNm as described in [4] (see also **Fig. 1**). This results in a contact pressure $p = 3200$ MPa and a contact force $Q_{\max} = 50243$ N, which represents maximum pulsating load as shown in **Fig. 2b**.

The bearing rings are made of steel 42CrMo4 (AISI 4142). The material properties for each hardness in question (layer) are obtained on the basis of the data given in [6,7] and are shown in **Table 1**. They are determined whether by averaging values (E, b, c) or by using linear regression (R_m, ε_f , σ_f', ε_f'). These values are then used to design cyclic stress-strain curves according to the **Eq. (2)**. Depth-dependent hardness profile of a raceway and cyclic stress-strain curves for each layer are shown in **Fig. 4a** and **Fig. 4b**, respectively. Elastic in plastic Poisson's ratios for all layers are and $\nu_e = 0.3$ and $\nu_p = 0.3$, respectively.

Table 1: Material properties used for the FEM analysis

#	HB	E [GPa]	R_m [MPa]	ε_f	σ_f' [MPa]	b	ε_f'	c
core	280		1290	0.930	1555		0.712	
transition	445	205	1755	0.542	2040	−0.081	0.389	−0.716
case	615		2240	0.142	2540		0.057	

3.2. Finite element analysis setup

For the purpose of the finite element analysis the geometry of the raceway is somehow simplified according to the Hertzian contact theory [3] as shown in

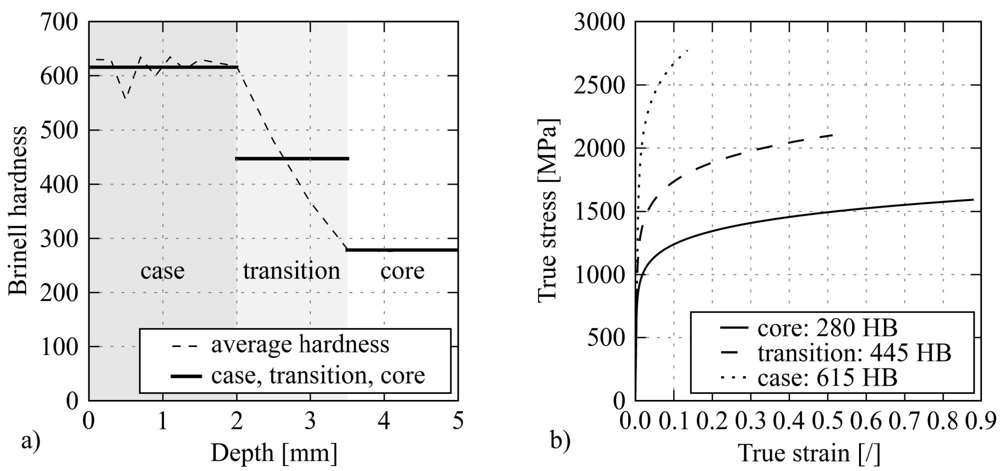

Fig. 4: Material properties of a raceway: a) depth-dependent hardness profile, b) cyclic stress-strain curves for each layer

Fig. 3b. Hence, the finite element model is able to take into account double symmetry boundary conditions. The raceway is divided into 3 layers with different elasto-plastic cyclic material properties. The bottom surface of the model is fixed. The contact force is applied in the reference point in the center of the ball and all the nodes on that surface are coupled to the reference point. The loading cycle consists of two steps. First, the contact force is increased to $Q_{\max}$, and second, the contact force is released. The stress and strain amplitudes are then calculated by subtracting appropriate values. The model is discretized using 8-node linear elements and the calculation is done using ABAQUS software.

4. Results and discussion

Results of the calculation are shown in **Fig. 5.** The figure shows equivalent mean stress $\sigma_{m,q}$ (**Fig. 5a**), maximal shear strain amplitude $\gamma_{a,\max}$ (**Fig. 5b**) and number of cycles to failure N_f (**Fig. 5c**) in relation to the depth z (see **Fig. 3b**). The figure also shows layers (case, transitional and core) and the depth at which the failure is suppose to occur.

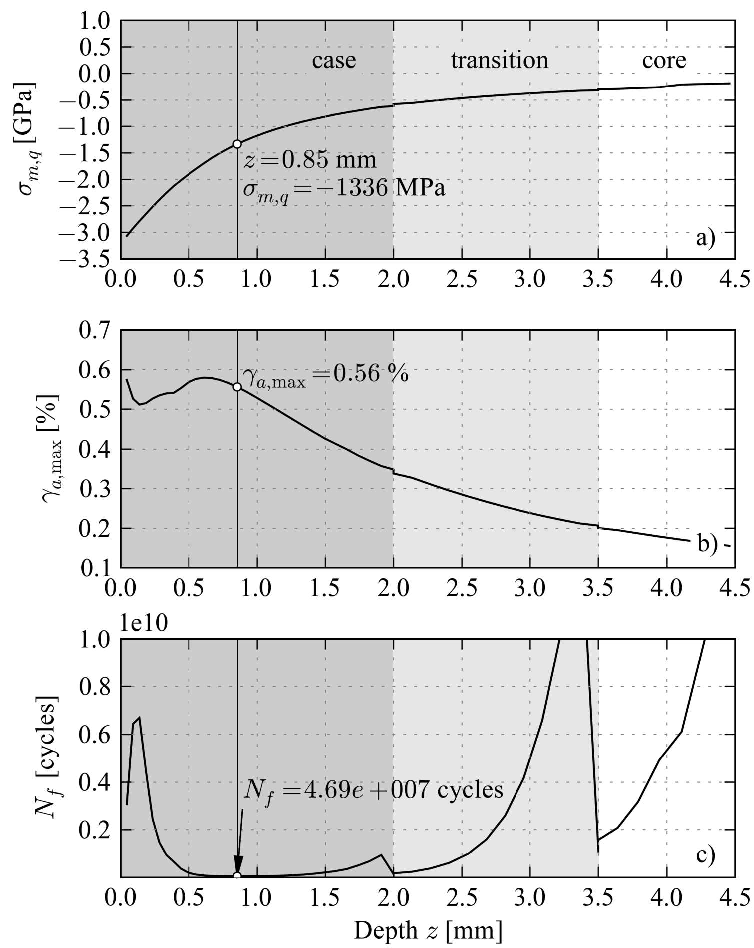

Fig. 5: a) Equivalent mean stress $\sigma_{m,q}$, b) maximal shear strain amplitude $\gamma_{a,\max}$ and c) number of cycles to failure N_f in relation to the depth z

The number of cycles needed for the failure to occur is $N_f = 4.96e7$ and the number of bearing revolutions is $N_r = 1.54e6$. The depth at which the failure is supposed to occur is $z = 0.85$ mm. **Fig. 5** shows that the failure occurs in the first, thus the hardest layer. Sudden changes of N_f at the layers' interfaces (see **Fig. 5c**) are a result of the stepwise changing of material parameters (see **Table 1** and **Fig. 4**).

The computations have also shown that at this contact load (Q = 50243 N) there is practically no plastic deformation of the raceway. Namely, the plastic deformation is less than 0.004%, which is negligible. Furthermore, Von Mises residual stress – i.e. stress at Q_{min} (after releasing Q_{max}) – is around 35 MPa, which is also practically negligible.

5. Conclusion

A computational procedure for calculation of fatigue life of large rolling bearings is presented. The calculation is based on the strain-life approach, and it takes into consideration depth-dependent elasto-plastic material properties of the bearing raceway. A practical example is presented for demonstration.

The presented approach seams to be fairly simple and yet provides a good basis for further development. In the future more attention should be paid to the modeling of the depth dependent material characteristics. Currently the changes are stepwise and rather coarse. This results in non-expected changes of number of cycles to failure in regard to the depth. The calculation of fatigue life would also be improved by taking into consideration kinematic hardening material properties. Furthermore, currently cyclic material characteristics for certain hardness are calculated on the basis of the characteristics available in the literature. Although these are taken from trusted sources, the calculation would most certainly benefit from using experimentally determined material properties.

References

[1] International Organization for Standardization, ISO 281:2007: Rolling bearings – Dynamic load ratings and rating life, ISO, 2007

[2] E. Zaretsky, L. Poplawski, and C. Miller, Rolling Bearing Life Prediction – Past, Present, and Future, National Aeronautics and Space Administration, 2000

[3] T.A. Harris, Rolling Bearing Analysis, John Wiley & Sons, 1991

[4] R. Potočnik, J. Flašker, and S. Glodež, Computational Model for Load Capacity of Large Slewing Bearings, in J. Pokluda (ed.), Multilevel approach to fracture of materials, components and structures, ESIS Czech Chapter, 2008, pp. 1887–1894

[5] R.I. Stephens, A. Fatemi, R.P. Stephens and H.O. Fuchs, Metal Fatigue in Engineering (Second Edition), John Wiley & Sons, 2001

[6] M. Bauccio, ASM Metals Reference Book, ASM International, 1993

[7] Information on http://www.fatiguecalculator.com (data retrieved from SAE J1099 report)
[8] M. Roessle, A. Fatemi, Strain-controlled fatigue properties of steels and some simple approximations, International Journal of Fatigue 22 (2000) 495–511
[9] J.H. Park, J.H. Song, Detailed evaluation of methods for estimation of fatigue properties ,International Journal of Fatigue 17 (1995) 365–373
[10] S. Glodež, J. Flašker, Dimenzioniranje na življenjsko dobo (in Slovene), University of Maribor, 2006